NATIONAL RADIO ASTRONOMY OBSERVATORY
SOCORRO, NEW MEXICO
VERY LARGE ARRAY PROGRAM

VLA ELECTRONICS MEMORANDUM NO. 181

MODIFICATIONS TO THE VLA FRONT ENDS FOR SOLAR OBSERVATIONS

J. W. Archer

April 1979

1.0 INTRODUCTORY REMARKS ON THE EXPECTED SYSTEM TEMPERATURES DURING SOLAR OBSERVING

The proposed modifications to the VLA front end are intended, initially at least, to enable solar observations to be made during the coming period of maximum solar activity. The expected brightness temperatures at different points on the solar disc can vary widely with angular position, and absolute values are not well determined. The antenna temperature at the feed terminals of a VLA antenna tracking a point near the center of the Sun depends upon the beam efficiency at the observing frequency, the power spectrum of the solar radiation and the distribution of bright point sources, corresponding to regions of enhanced solar activity, within the antenna beam.

Clearly the antenna temperature will be related strongly to the observing frequency, the degree of solar activity and beam position relative to the solar disc - it is for these reasons that only relatively vague estimates of the expected antenna temperature can be given as a guide for system design. Drift scan measurements with two VLA antennas on different days indicated the antenna temperatures summarized in Table I. The measurements taken January 21, 1979 show signficant enhancements corresponding to regions of increased solar activity, whereas those of January 25, 1979 indicate that the enhancements had significantly diminished in amplitude. These values compare favorably with the theoretical

predictions of Appendix (i). Table II lists the theoretical beam efficiency and the derived mean and peak solar brightness temperatures observed.

TABLE I

Band	Antenna Temp. (^{o}K) Peak	Mean Background	Comments
L	$5 \cdot 5 \times 10^{4}$	---	Sun unresolved
C	$3 \cdot 0 \times 10^{4}$	$2 \cdot 0 \times 10^{4}$	
U	$1 \cdot 4 \times 10^{4}$	$0 \cdot 8 \times 10^{4}$	
K	$1 \cdot 0 \times 10^{4}$	$6 \cdot 0 \times 10^{3}$	

TABLE II

Band	η_B (typ.) (30 arcseconds source diameter)	T_B (mean)	T_B (peak)
L	.30	--	183,000
C	.65	31,000	46,000
U	.64	12,500	22,000
K	.52	11,500	19,000

The corresponding nominal system input noise power spectral density is indicated in Table III, where the geometric mean of peak and background values have been taken for the assumed solar brightness.

TABLE III

Band	Noise Power Spectral Density at Receiver Input (includes receiver contribution)
L	-63·79 dBm/550 MHz
C	-67·30 dBm/550 MHz
U	-70·38 dBm/550 MHz
K	-71·90 dBm/550 MHz

Even though those values can be expected to vary by at least ±5 dB depending upon solar activity and beam position relative to the disc, they represent a reasonable starting point for a design analysis. The nominal power at the input to the F6 module lies in the range -44 dBm to -4 dBm in 550 MHz bandwidth for correct operation of the F4 ALC loop (with F6 in normal insertion loss mode of -15 dB). Over this range the F4 ALC attenuator exhibits a transmission phase variation of about $\pm 7{\cdot}5^{\circ}$. Total gain between feed and F6 input is given in Table IV, together with the value of attenuation which must be introduced in the amplifier chain to maintain the nominal F6 input at -30 dBm/550 MHz.

TABLE IV

Band	Overall Receiver Gain (dB)	Gain Reduction (dB)
L	68	34·2
C	65	27·7
U	61	20·6
K	60	18·1

The required nominal calibration noise source injection levels, fixed at about 10% of the nominal quiet Sun system temperature are given in Table V.

TABLE V

Band	Cal. Temp. (Nom.)	Band	Cal. Temp. (Nom.)
L	4500 K	U	800 K
C	2000 K	K	600 K

2.0 ALTERNATIVE METHODS FOR REDUCING RECEIVING SYSTEM GAIN

As a preliminary, it is helpful to list a few relevant receiver parameters related to maximum signal power handling capability of various elements of the receiver chain. Table VI summarizes those values.

TABLE VI

Device	3 dB B.W.	Gain	Noise Figure	Minimum 1 dB Gain Comp. (output)	Second Order Intercept Point
Paramp	~550 MHz	26 dB	0·3 dB	-28 dBm (broadband noise)	Harmonic Products insignificant below saturation.
GaAs FET	~550 MHz	41 dB	3·0 dB	0 dBm (broadband noise)	+20 dBm

From Section 1.0, Table IV lists the necessary reduction in amplifier gain to maintain nominal F4 input power levels. It is

clear, that without this gain reduction prior to the GaAs FET stage, saturation may occur in the output of this amplifier. The gain reduction can be implemented in a number of ways.

2.1 Defocussing Antenna Feed System

A reduction in the effective gain of a paraboloidal antenna system can be achieved by an axial defocussing of the feed. Then the effective system temperature at the receiver input is reduced when observing the Sun by an amount proportional to the gain reduction and the RF amplifier stages are not overdriven.

In the case of a Cassegrain geometry a small movement of the subreflector corresponds to a relatively large axial displacement of the feed phase center.

$$\Delta\mathcal{D}_{eq} \sim \frac{-F_m F_e}{L_v^2} \Delta\mathcal{D}$$

Where $\Delta\mathcal{D}_{eq}$ is the equivalent feed displacement,

$\Delta\mathcal{D}$ is the subreflector displacement,

L_v is the separation between subreflector apex and main dish focal point ($\Delta\mathcal{D} << L_v$),

F_m is the main dish focal length,

F_e is the distance from feed phase center to main dish focus.

Ingerson et al. (1973) give a theoretical analysis of the effect on gain and beam power pattern of an axial displacement of the feed. For on-axis gain reductions of the required order (~25 dB @ 6 cm) and uniform aperture illumination, as is the case with the VLA antennas, an effective feed displacement of about $1{\cdot}8\ \lambda_o$ is required. However, under this condition, the beam power pattern assumes a highly undesirable distribution as indicated in Figure 1.

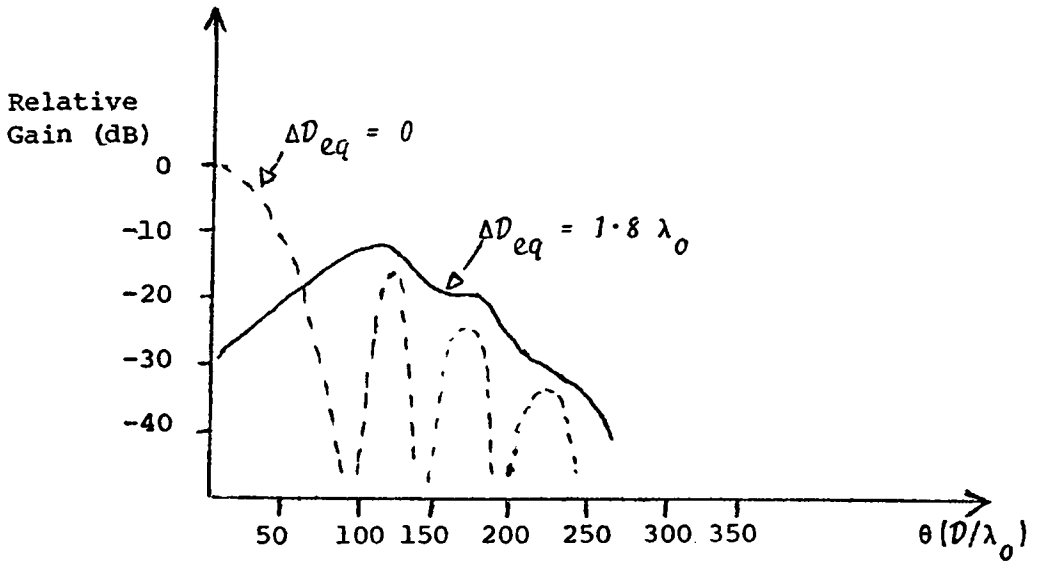

Figure 1: Axially Defocussed Beam Patterns for a VLA Antenna

Hence, even though the method appears attractive since receiving system noise figure is not degraded, the beam pattern distribution renders the approach undesirable.

2.2 Attenuator Inserted Between Feed and Receiver

Inserting a switchable waveguide attenuator between feed and receiver is another alternative. In this case the receiving system temperature is increased to a level where $T_{REC} \sim T_{ANT}$ for solar observing. The minimum detectable brightness temperature variations in the synthesized map is then approximately doubled, when compared to the case where $T_{REC} << T_{ANT}$

$$\Delta T_{B_{min}} \propto \frac{\sqrt{T_1 T_2}}{\eta_s \sqrt{B \Delta t}}$$

where T_i is the T_{SYS} of the i^{th} receiver,

B is the bandwidth,

Δt is the integration time,

η_s is the synthesized beam efficiency.

Furthermore, the insertion loss of such an attenuator, when in the low insertion loss state may add significantly to the system temperature for cosmic observing.

2.3 Turning Off the Parametric Amplifiers

The parametric amplifiers may be turned off by removing the pump drive with a suitable waveguide switch. In the off-state, the insertion loss of the paramps is of the order of -4 dB at a temperature of 15 K, hence T_{REC} ~ (C-band) 320 K. In this case, the gain reduction is about 30 dB, resulting in a power spectral density at the GaAs FET output of about -32 dBm/550 MHz at C-band for solar observing (quiet Sun).

2.4 Inserting a Switchable/Variable Attenuator After the Parametric Amplifier

In this case, the value of attenuation can be selected as desired to optimize the F4 input levels. In fact, the F4 ALC loop control could be transferred to a variable attenuator at this point in the amplifier chain for solar observing. A nominal attenuator value of 25 dB will degrade the receiver temperature to about 480 K at C-band. In the low insertion loss state, the maximum insertion loss would be 1 dB, resulting in a receiver temperature increase of less than 1 K at C-band.

On the basis of the foregoing discussion it appears that alternatives 2.3 and 2.4 offer the most viable approach from a purely signal level oriented point of view.

3.0 CALIBRATION

3.1 T_{SYS} for Individual Receiver

Alternatives 2.3 and 2.4 only will be considered here. Table V listed the required calibration temperatures when the

antenna temperature close to solar radiation predominates the system temperature. Table VII lists current typical calibration insertion coupler values, noise source ENR's and nominal calibration insertion temperatures.

TABLE VII

Band	Coupler (dB)	ENR (dB)	T_{CAL} (^{o}K)
L	-25	26	1·4
C	-30	25	1·5
U	-30	25	6·5
K	-30	24	7·5

To achieve the desired calibration levels for solar observing, assume -17 dB couplers are installed for each band. The increase in system temperature due to the tighter coupling value will certainly be significant at the lower frequency bands. However, if the revised calibration scheme is implemented on only one or two antennas, the degradation may be acceptable for the array in general. Then, the desired noise source ENR's at the coupler inputs are given in Table VIII.

TABLE VIII

Band	Required ENR (dB)	Maximum Available ENR (dB)
L	28·90	32
C	25·40	31
U	21·44	31
K	20·20	30

Each noise source normally in use has a 6 dB attenuator installed between diode and output connector. With this attenuator removed, the available ENR with VLA sources is as indicated in Table VIII, at the output of each source. It appears that at K- and U-bands a 4-way power divider can be used with switchable attenuator and a single source for both cosmic and solar observing. The power divider outputs would connect in the normal mount to the couplers for the AC and BD channels of the K- and U-band receivers. However, at L- and C-bands, more than one noise source is required. At L-band it appears desirable to use separate sources, one for each of the AC and BD channels of the L-band receivers. At C-band a single noise source with power divider should be used. A typical switchable calibration schematic, allowing selectable normal or solar observing, is shown in Figure 2.

The available calibrated dynamic range for solar observing is then limited by the ratio of T_{SYS} to T_{CAL}. Typical offsets in the synchronous detector circuitry limit the minimum reliably usable synchronous detector output voltage to about 0·5 volts. If the nominal synchronous detector output voltage is 5·0 volts, the available dynamic range, for increasing total power, is 10 dB.

3.2 Amplitude and Phase Calibration (Synthesis Telescope)

To be able to observe calibration sources, a facility must exist which enables the receiving system to revert to normal observing mode. Furthermore, the changes in the phase responses of each receiver between normal and solar mode must be well defined to enable calibration to be effective. If alternative 2.3 is used to implement the solar observing mode, the change in receiver gain is relatively well defined, but the change in transmission phase is not well determined due to the change in

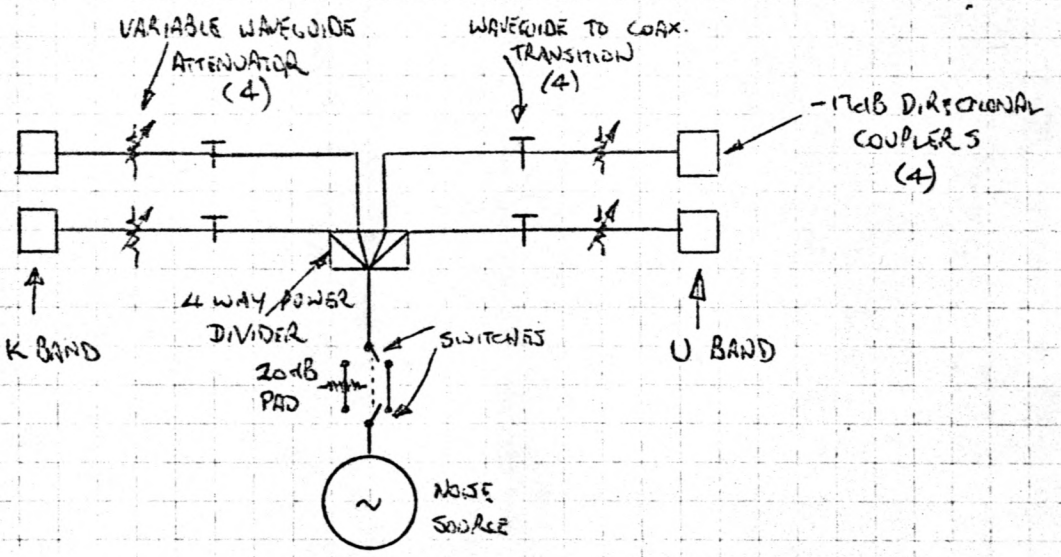

K & U BAND CALIBRATION SCHEME.

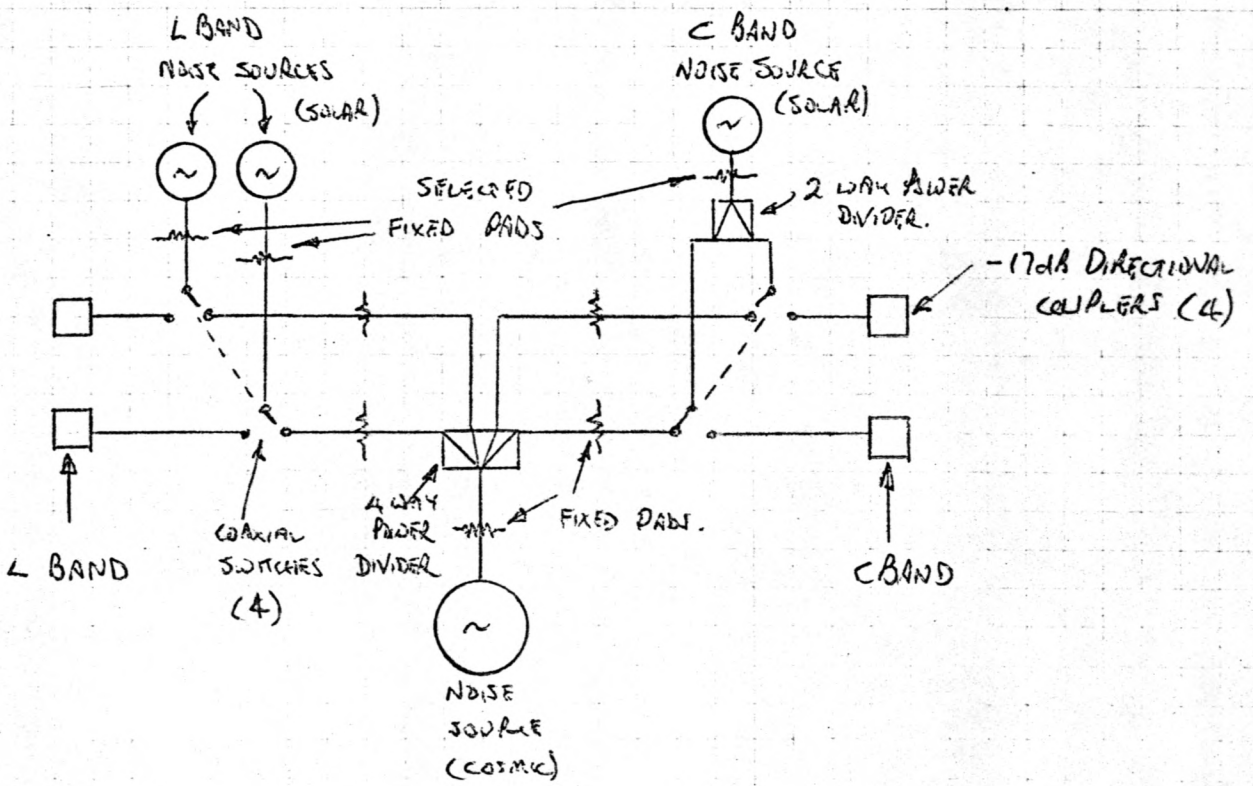

L & C BAND CALIBRATION SCHEME.

FIGURE 2

operating point of the F4 ALC attenuator. Therefore, there remains an uncalibrated phase uncertainty of the order of tens of degrees when using the instrument in this mode.

In the case of alternative 2.4, however, the switchable/variable attenuator can easily be designed to have phase shift variations of less than $\pm 5^{o}$ within a 10% bandwidth over the full attenuation range (~-5 to 40 dB). Furthermore, the inserted attenuation value at each band can be selected to hold the F4 ALC operating point near the nominal value.

4.0 RECOMMENDATIONS

Alternative 2.4 is recommended as the most attractive approach for the long term. Initially, a switched attenuator (fixed) should be used with a value of 25 dB. The resultant nominal power levels at the F6 module input are then as in Table IX. The minimum available dynamic range (L-band observing) before 1 dB compression in the GaAs FET amplifier is of the order of 25 dB. At a later date selectable attenuation values for each band could be implemented in order to reduce the affect of F4 ALC loop operating point vs transfer phase depending on system phase when switching from normal to select mode.

TABLE IX

Band	F6 Input Power in 550 MHz B.W.
L	-20·8 dBm
C	-27·3 dBm
U	-34·4 dBm
K	-36·9 dBm

The T_{SYS} calibration scheme of Figure 2 is recommended for

implementation on two antennas only. These should be used as a transfer standard for T_{SYS} correction of all other receivers in the array. This technique is viable since the antenna temperature due to solar radiation dominates the intrinsic receiver temperature at all bands. It assumes, however, that beam efficiencies of all antennas are identical at each observing frequency.

Concerning costs, consider first the switchable attenuator. Two are required per antenna, for each operational antenna.

Alternative 1: Mechanical Coax Switches and Fixed Pads

Coax switch - 4 required/antenna @ $100 each

Pads - 2 required/antenna @ $35 each

Total cost per antenna approximately $500.

Alternative 2: Commercial Pin Absorptive Attenuators

2 required per antenna @ $425 each

Total cost per antenna approximately $900.

Alternative 3: In-house Manufactured Absorptive Attenuators (Design available)

Pin diodes - 4 required/antenna @ $15 each (minimum)

P.C. mask and etching - 1 required/antenna @ $65 each

Connectors - 5 required/antenna @ $15 each

P.C. board material - 1 required/antenna @ $20 each

Total cost per antenna $220 maximum.

Alternative 3 is recommended on the basis of this analysis. All circuit board material is available in-house and complete design analysis has been undertaken.

An approximate estimate of the cost of the switchable calibration scheme for one antenna is:

L- and C-bands:	4 switches @ $100 each 3 noise sources @ $400 each 4 couplers @ $670 (L-band x 2) @ $320 (C-band x 2)	Total: $3580

K- and U-bands: 2 switches @ $500 each
4 couplers @ $250 each
} Total: $2000

For the short term alternative 2.3 is the easiest and cheapest to implement. Various methods for turning off the parametric amplifiers are currently under investigation. For the present solar maximum period, therefore, solar operation will be with parametric amplifiers turned off and the revised calibration scheme implemented on two antennas only.

REFERENCE

Ingerson, P. G. and Rusch, W. V. T., IEEE Trans. Ant. Prop. AP-21, pp. 104-106, Jan. 1973.

APPENDIX (i)

EXPECTED ANTENNA TEMPERATURE FOR THE VLA DURING THE SOLAR MAXIMUM

The temperature of the quiet Sun ranges from ~1.5×10^5 K at 21 cm to less than ~10^4 K at 1.3 cm. The antenna temperature of the VLA for the quiet Sun will be highest at 21 cm where it will range between 3×10^4 to 7.5×10^4 K (depending on the beam efficiency and the antenna pointing) to less than ~1.5×10^4 K at all the shorter wavelengths. However, the largest contribution to the antenna temperature during the solar maximum will be from active regions on the Sun. The observed flux of active regions has a large spread but has typical values of the order of 100 sfu (1 solar flux unit - 10^{-22} w $m^{-2}s^{-1}$) at 21 cm. The spectrum of the sources is nonthermal and so the flux at shorter wavelengths is less. As shown below, the antenna temperature for a 100 sfu source is ~7.5×10^4 K. Assuming a typical spectrum for active regions we expect typical antenna temperatures to be:

Frequency	Expected Antenna Temperature
1.4 GHz	10^5 K
5 GHz	7.5×10^4 K
15 GHz	3×10^4 K
22 GHz	2×10^4 K

Note that we expect these temperatures only when there are strong active regions on the Sun. When there are no such regions, the expected antenna temperature will be much less, ranging from around 5×10^3 K at 1.3 cm to ~5×10^4 K at 21 cm.

APPENDIX (ii)

ANTENNA TEMPERATURE FOR THE VLA FOR AN ACTIVE REGION OF 100 sfu SOURCE

Antenna temperature $T = \frac{SA}{2k} \times \eta$

$= \frac{10^{-20} \times 421}{2 \times 1.38 \times 10^{-23}} \eta$

$= 1.5 \times 10^5 \eta$

η = efficiency

$S = 10^2$ sfu $= 10^6$ Jy

$= 10^{-20}$ s/m^2/s

$A = 421$ m^2

$k = 1.38 \times 10^{-23}$ J/k

$\eta = .5$ 21 cm

$= .65$ 6 cm

$= .54$ 2 cm

$= .46$ 1.3 cm

taking typical value of 0.5

$$T_{ANT} \approx 7.5 \times 10^4 = 75,000 \text{ K}$$

At 21 cm antenna temperature due to the quiet Sun is between 30,000 to 75,000 K (depending on the beam efficiency and pointing) but at higher frequencies the quiet Sun contribution is <15,000 K and so can be ignored compared to active region.

NATIONAL RADIO ASTRONOMY OBSERVATORY
SOCORRO, NEW MEXICO
VERY LARGE ARRAY PROGRAM

ADDENDUM TO VLA ELECTRONICS MEMORANDUM NO. 181

MODIFICATIONS TO THE VLA FRONT ENDS FOR SOLAR OBSERVATIONS

J. W. Archer

August 1979

1.0 INTRODUCTION

This paper gives further consideration to the problems involved in making possible solar observations with the VLA. Electronics Memorandum 181 proposed the installation of a switchable attenuator as a possible method for decreasing receiver gain when observing the sun. This method has now been adopted. This paper gives results of an analysis aimed at determining the optimum value for the reduction in gain, taking into account possible departures of receiver system gain and system temperature from the nominal values. The quiet sun is used as a basis for the analysis. However, the results may readily be applied to the case where other values of solar flux are to be used as a design reference. It is shown that, using the switchable attenuator, quiet sun observations are feasible, with possibly acceptable phase calibration transfer accuracy by observing normal VLA calibrators. Phase calibration accuracy is degraded when the system temperature for solar observing departs markedly from the nominal design values.

2.0 THE SWITCHABLE ATTENUATOR

Figure 1 shows a block diagram of a VLA antenna receiver system, indicating the proposed location of the switchable attenuator for solar observing. The attenuator comprises a pair of electromechanical coaxial single-pole double-throw switches interconnected as shown in Figure 2. The electrical lengths of the two alternate paths

between switches are adjusted to be equal to within ±0.2 degrees of phase at 4.75 GHz. The switches are of fail-safe design, reverting to the low insertion loss condition if the actuating current is disconnected. The insertion loss in the low insertion loss state is 0.2 dB±0.1 dB.

3.0 THE CHOICE OF ATTENUATOR VALUE

Figure 1 indicates the approximate tolerances on the gains of the components comprising the receiver subsystems. Since the F4 ALC loop is designed to hold the output power from the complete system at a constant value of -34.0±0.5 dBm, the variations in gain or variations in system temperature cause the ALC attenuator to operate at a different insertion loss for each individual antenna system and even for different channels at the same antenna. Figure 3 shows the maximum (worst case) variation in ALC attenuator operating point for all four VLA receiver bands. The nominal operating insertion loss is -12 dB, although, clearly, substantial departures from this condition are feasible.

The ALC attenuator introduces a phase shift which varies with its insertion loss, and hence, the system temperature. The PIN diode attenuators used in the VLA receivers are state-of-the-art devices designed to minimize the effect over as large a dynamic range as possible. However, as can be seen from Figure 4, large departures from the nominal operating point can induce significant excess phase shifts. The situation is complicated by the presence of some attenuators with markedly different characteristics as can be seen from the Figure.

The main reason for using a switchable constant phase attenuator for solar to normal mode switching is to enable array phase calibration using normal VLA calibration sources. Every effort must therefore be made to see that the F4 ALC attenuator insertion loss remains, as nearly as possible, unaltered when switching from normal to solar observing conditions.

As stated previously, the present analysis will be based on optimum accuracy for phase calibration transfer when observing the quiet sun. This analysis may easily be adopted to other source flux densities if desired. Table I gives nominal quiet sun antenna temperatures for the VLA, and the ratio of quiet sun system temperature to nominal normal mode T_{sys}.

TABLE I

Band	T_{sys} (Normal)	T_{sys} (Quiet Sun)	Ratio
L	50 K	4.5×10^4 K	29.54 dB
C	50 K	2.0×10^4 K	26.02 dB
K_u	300 K	8×10^3 K	14.26 dB
K	300 K	6×10^3 K	13.01 dB

Two cases will be considered. The first uses a fixed switchable 16 dB attenuator in the solar/normal mode switch in conjunction with F6 attenuation settings of:

Normal: -12 dB;

Low: -18 dB.

At L- and C-bands the F6 is set to low gain mode for solar observations. The F6 phase change can be calibrated using normal calibrators at high and low gain settings. The 4 dB change can be handled under all tolerance conditions by the F4 ALC loop, as can be seen from Figure 3.

Figure 5 shows the resultant phase calibration transfer errors for quiet sun observations and nominal normal mode T_{sys} as a function of normal mode F4 ALC attenuator operating point. In general, errors are less than 3°±1.5° at C-, K_u- and K-bands for all operating points greater than 8 dB. At L-band, performance is somewhat poorer. Figure 6 illustrates the transfer phase calibration accuracy for a system temperature during solar observations of 20 dB above the nominal quiet sun. For K_u- and K-bands errors are generally less than 10°±5°, whereas for L- and C-bands errors can exceed 20° and insufficient ALC operating range is evident.

As a second case, consider F6 attenuation settings of:

Normal: -12 dB;

Low: -20 dB.

with a switchable attenuator high insertion loss state of -18 db. In this case, F6 phase calibration may be achieved in a similar fashion to that previously described. However, marginal operation of the ALC loop may be encountered in some cases. Figure 7 shows phase transfer accuracy in this case for L- and C-bands. Figure 7 also indicates the affect of variations in normal observing mode system temperatures on predicted phase accuracy. In general, the approach used here results in improved phase accuracy at L- and C-bands - better than 2°±1.5° for normal ALC attenuator operating points of greater than 8 dB. As can be seen from Figure 8, dynamic range is also improved with phase errors for system temperatures 20 dB above quiet sun being generally less than 15°±5°.

Within ±3 dB of the nominal ALC attenuator operating point and with nominal normal mode T_{sys}, quiet sun transfer errors are typically less than 3° at all four observing bands. For a source at 20 dB above quiet sun, these errors are typically less than 10° at C-, K_u- and K-bands, and less than 15° at L-band.

4.0 DYNAMIC RANGE CONSIDERATIONS

The usable dynamic range is primarily restricted by the minimum calibration signal-to-system temperature ratio. The injected calibration noise power must be 10% of the minimum expected system temperature - a cal. signal stronger than this may cause problems in the operation of the correlator when observing a source such as the sun for which relatively high cross-correlation coefficients may occur at the shorter antenna spacings. On this basis, the dynamic range is restricted to approximately 13 dB above the quiet sun.

If saturation of a component in the receiver system is considered as the limiting factor, then the dynamic range relative to the quiet sun is approximately 20 dB. The restriction here is imposed by the first amplifier stage of the F4 module, which enters the 1 dB gain compression region with a module input power of about -30 dBm.

5.0 RECOMMENDATIONS

The recommended solar observing configurations are as follows:

Case i) Quiet Sun Observing

a) Injected calibration noise temperature equal to 10% of quiet sun system temperature.

b) Switchable, constant phase attenuator with insertion loss states of:

Low: -0.2 dB; High: -18 dB.

c) F6 module insertion loss states set to:

Low: -12 dB; High: -20 dB.

Case ii) Best Compromise For Quiet and Active Sun

As outlined in the communication of Kundu and Rao included as appendix (i) of Electronics Memorandum No. 181, this compromise results in antenna temperatures varying from approximately 3 dB above the quiet sun values at 21 cm to 6 dB above quiet sun at 1.3 cm.

a) Injected calibration noise temperature equal to 10% of quiet sun system temperature.

b) Switchable constant phase attenuator with insertion loss states of:

Low: -0.2 dB; High: -20 dB.

c) F6 module insertion loss states set to:

Low: -12 dB; High: -20 dB.

In this case, when observing the quiet sun, calibration phase errors of about 5° can be expected. In addition, the output of some of the receivers in the array may no longer be adequately leveled. For observations of active regions which result in the antenna temperatures specified by Kundu and Rao, phase calibration transfer errors should not exceed 3°.

A practical proposition for future consideration might be a "binary"-step, constant phase attenuator using pin diode switches and chip attenuators in a microstripline configuration. This device would replace the fixed attenuator in the presently recommended system. Three steps might be sufficient to handle a wide range of solar ob-

serving possibilities - 4, 8, 16 dB - and the device should be easier and more feasible to construct than the constant phase pin diode current-controlled attenuator originally proposed in Electronics Memorandum 181.

6.0 ACKNOWLEDGMENT

The author would like to thank L. R. D'Addario for useful discussions and the provision of the material for Figures 1 and 3.

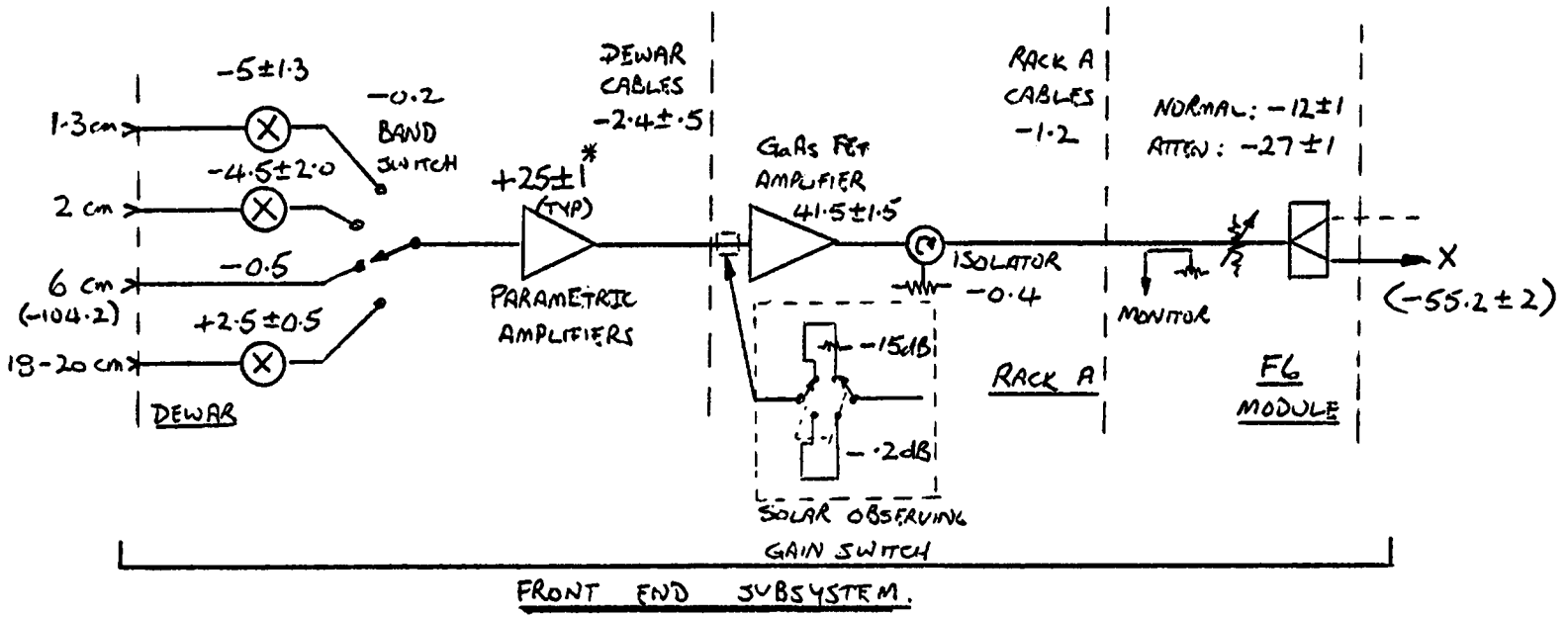

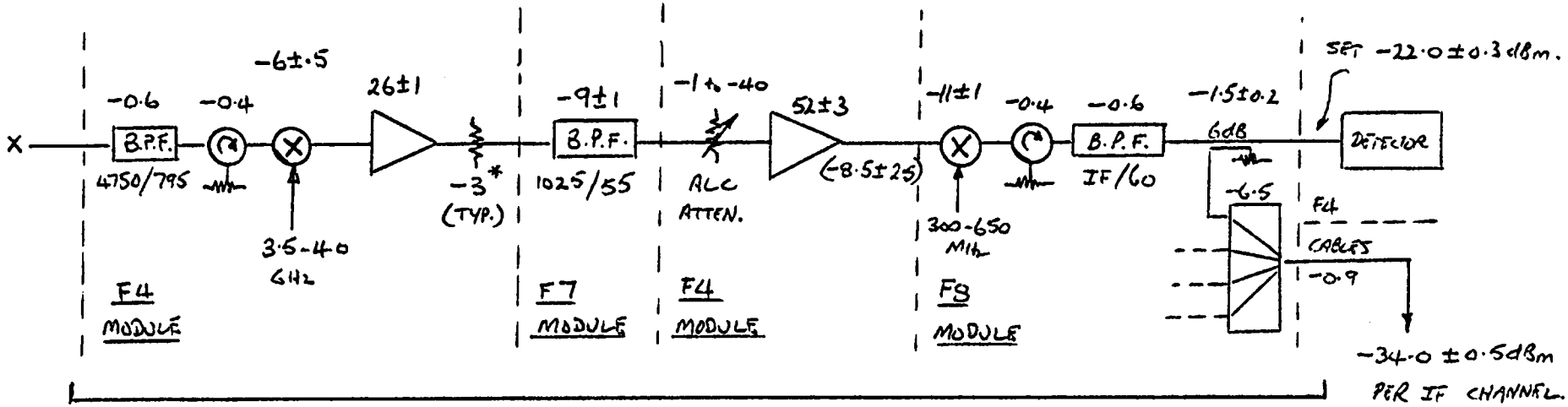

FIGURE 1.

VLA ANTENNA RECEIVER SUBSYSTEMS.

GAINS, TOLERANCES AND POWER LEVELS.

NOTE: THIS DATA IS APPROXIMATE ONLY. VALUES MARKED * ARE SELECTED OR ADJUSTED IN SERVICE. TYPICAL VALUE ONLY IS GIVEN.

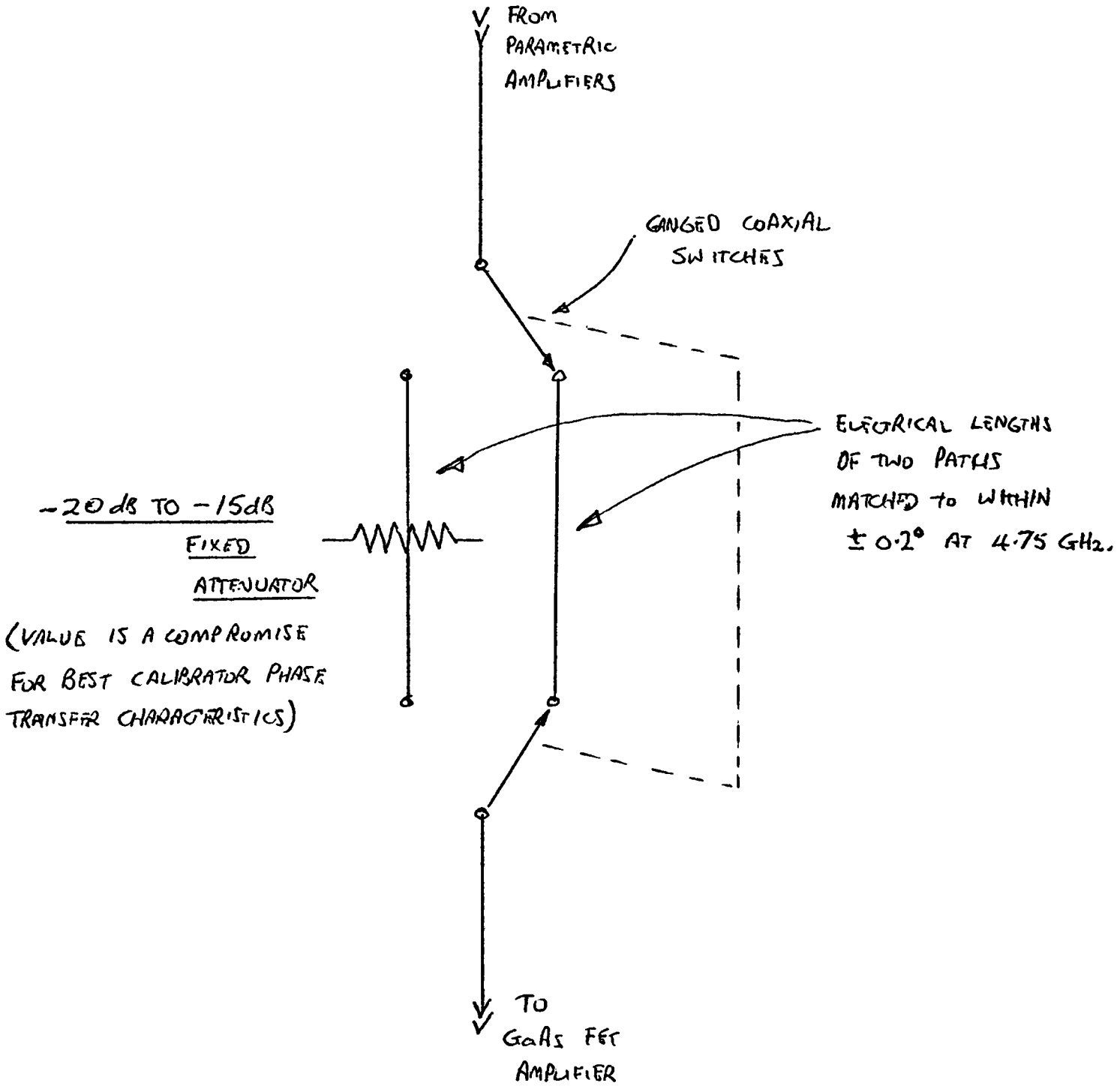

FIGURE 2

SOLAR MODE GAIN SWITCH SCHEMATIC

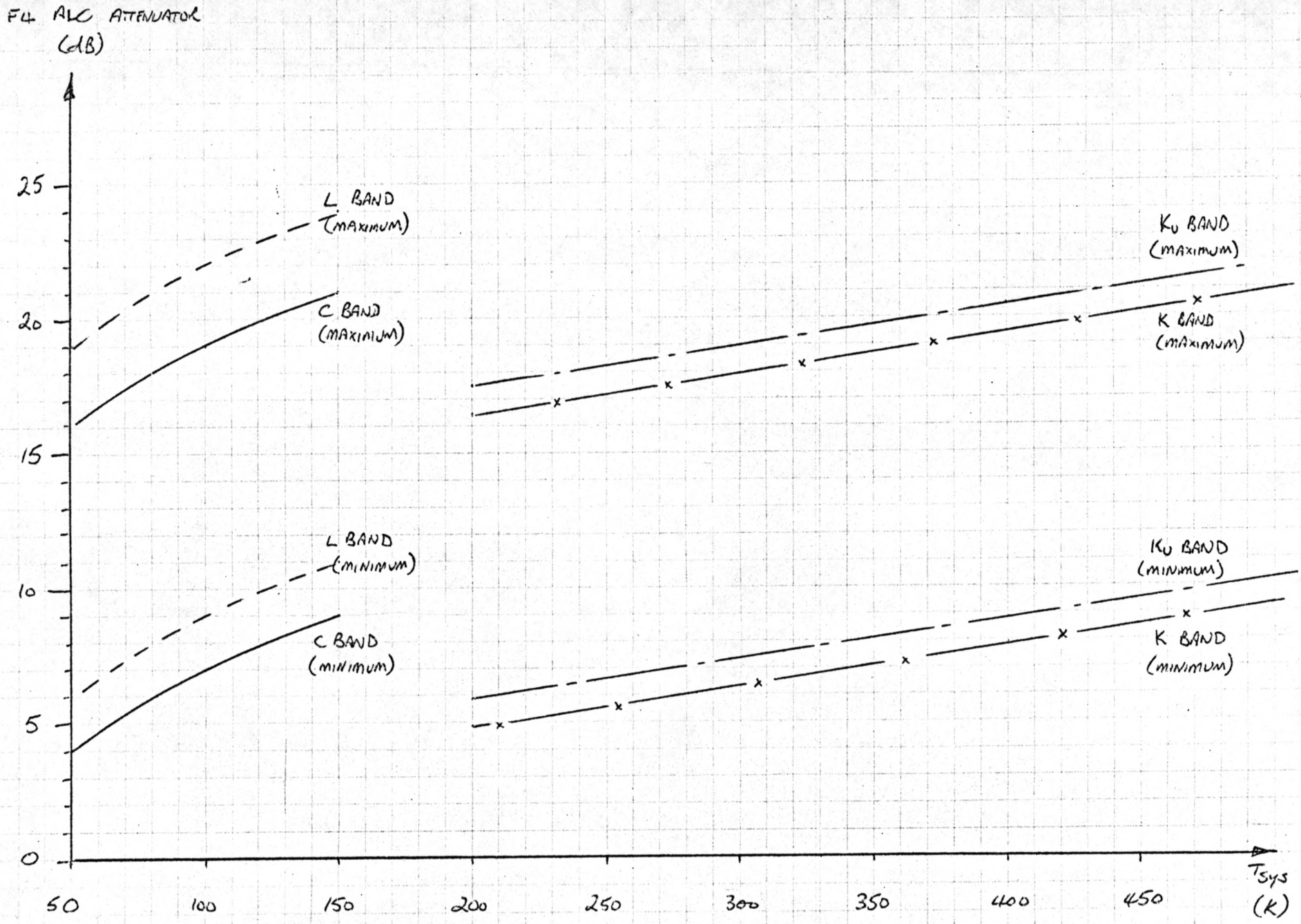

FIGURE 3 RANGES FOR F4 ALC ATTENUATOR INSERTION LOSS FOR VARYING T_{SYS} AT DIFFERENT BANDS.

(TAKES ACCOUNT OF WORST CASE RECEIVER GAIN VARIATIONS)

NOTE: THIS DATA HAS BEEN DERIVED FROM MANUFACTURERS TEST INFORMATION ON THE UNITS WITH SERIAL NUMBERS INDICATED. SPECIFICATION A1318-N3 REQUIRES FOR THIS ATTENUATOR THAT THE PHASE VS ATTENUATION RESPONSE SHALL NOT EXCEED

i) IN RANGE 0 to 30 dB 1·5°/dB

ii) IN RANGE 10 to 20 dB 0·5°/dB

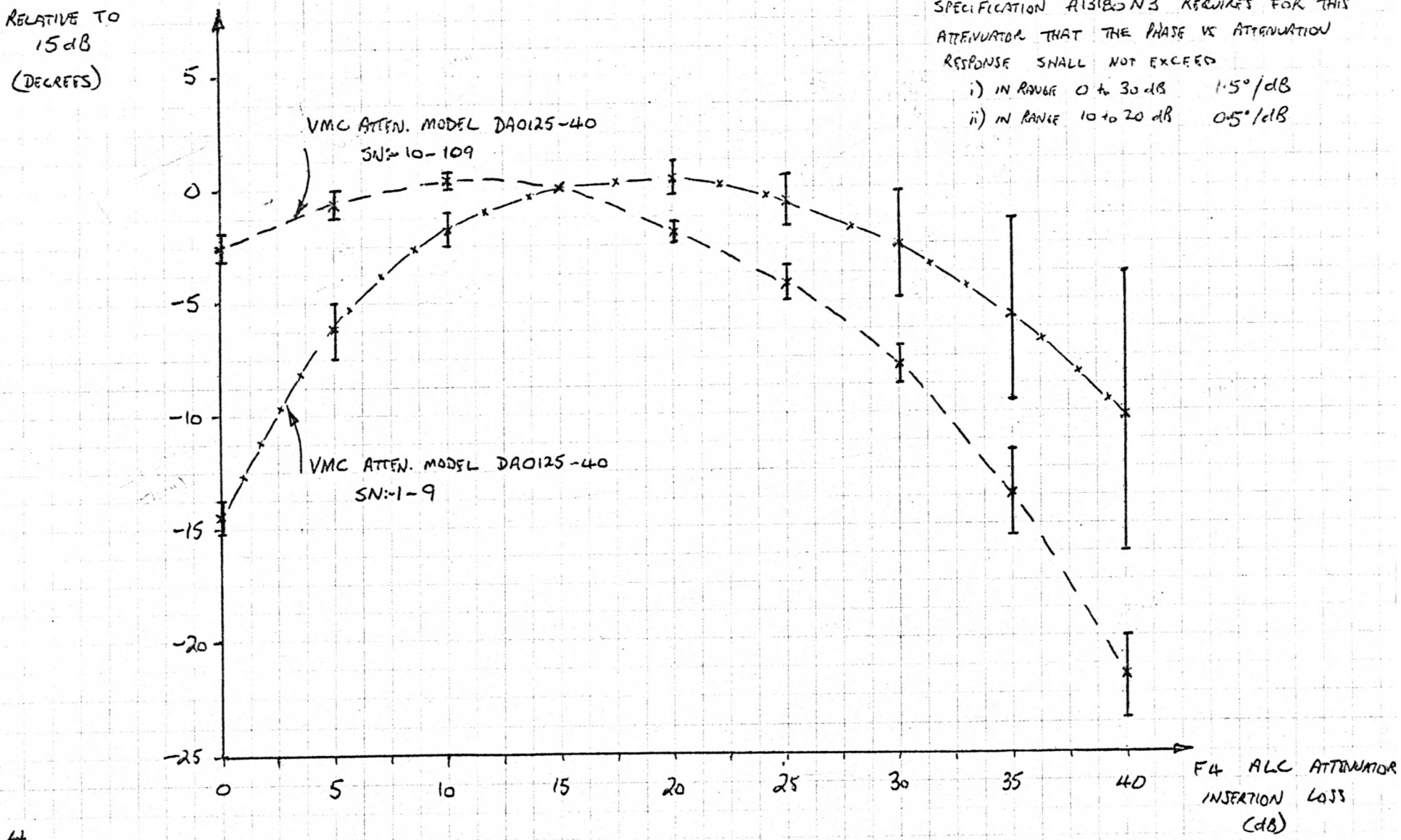

FIGURE 4

RELATIVE INSERTION PHASE OF F4 ALC ATTENUATOR AS A FUNCTION OF INSERTION LOSS

BARS SHOW STANDARD DEVIATION OF SERIAL NUMBER GROUP FROM MEAN PHASE SHIFT

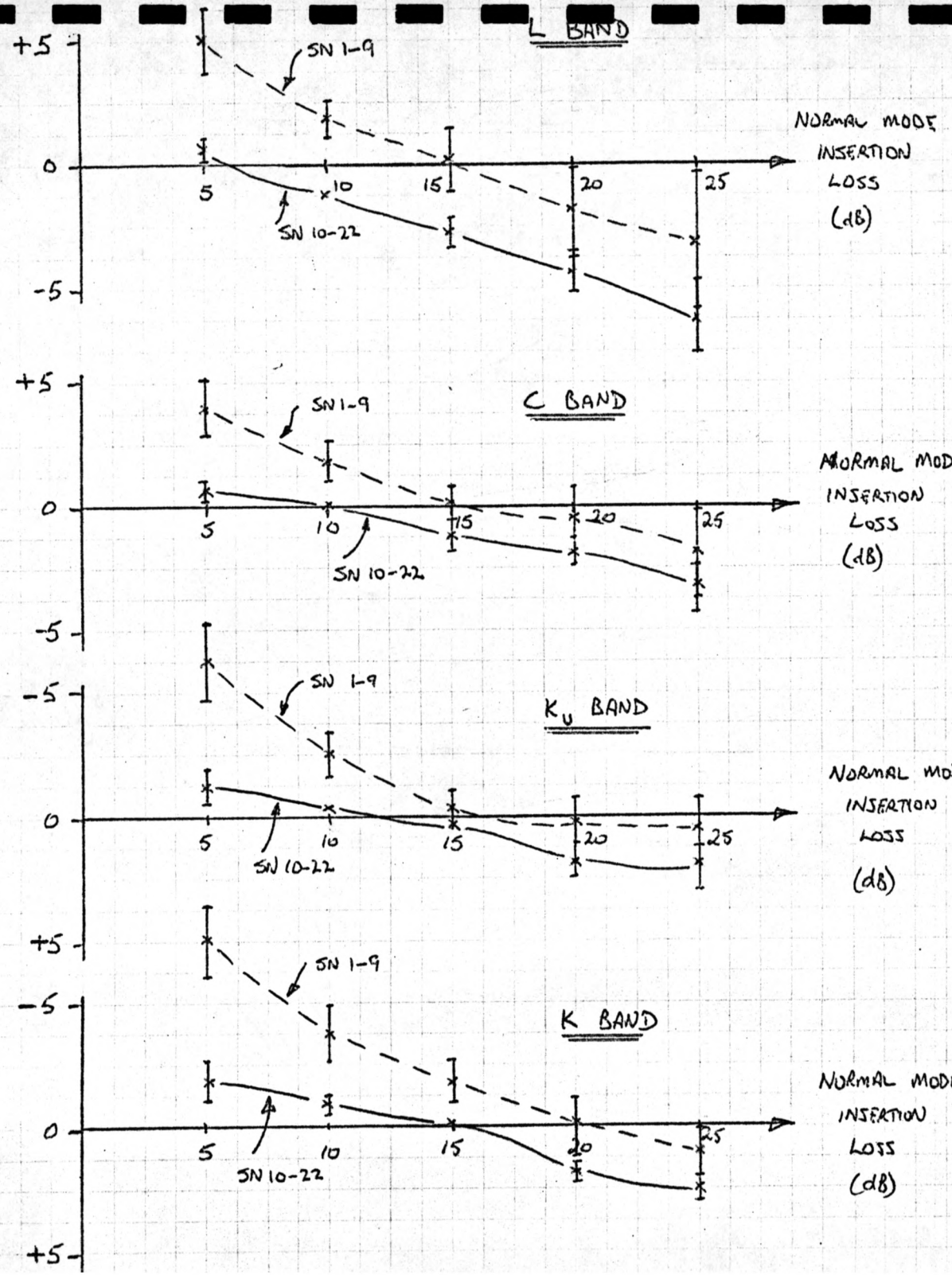

FIGURE 5

CALIBRATOR TO QUIET SUN PHASE TRANSFER ERROR FOR ONE ANTENNA AS A FUNCTION OF INITIAL NORMAL FL ALC ATTENUATOR INSERTION LOSS.

L+C BAND PAD = 22dB

K_U+K BAND PAD = 16dB

T_{SYS} = T_{SYS} (NOMINAL)

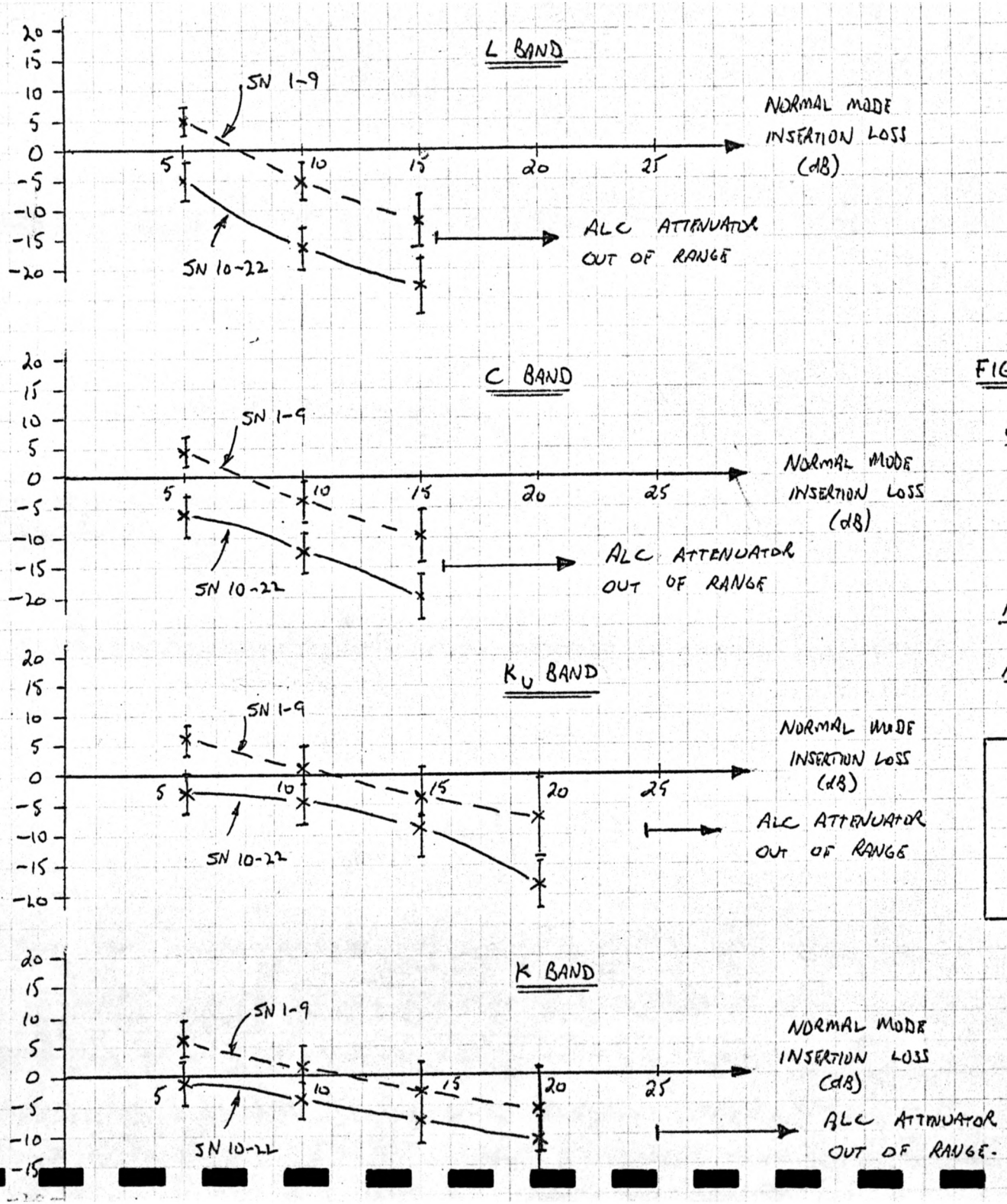

FIGURE 6

CALIBRATOR TO 20dB ABOVE QUIET SUN PHASE TRANSFER ERROR FOR ONE ANTENNA AS A FUNCTION OF INITIAL NORMAL FL ALC ATTENUATOR INSERTION LOSS.

L & C BAND PADS = 22dB

K_U & K BAND PADS = 16 dB.

$T_{S/S} = T_{S/S}$ (NOMINAL)

FIGURE 7

CALIBRATOR TO QUIET SUN PHASE TRANSFER ERROR FOR ONE ANTENNA AS A FUNCTION OF NORMAL FL ALC ATTENUATOR INSERTION LOSS

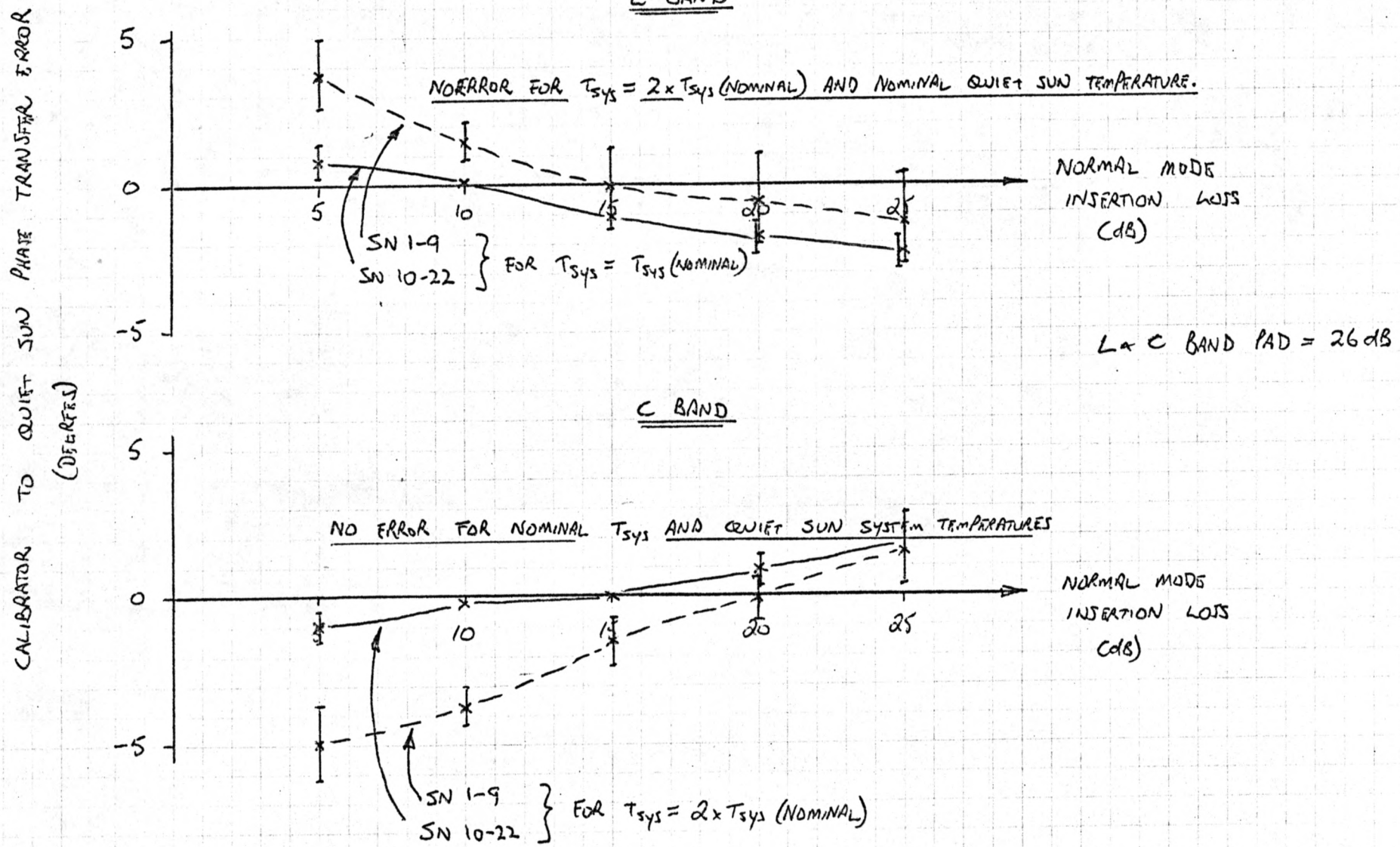

FIGURE 8

CALIBRATOR TO 20dB ABOVE QUIET SUN PHASE TRANSFER ERROR AS A FUNCTION OF NORMAL F4 ALC ATTENUATOR INSERTION LOSS.